

WeldMon: A Cost-effective Ultrasonic Welding Machine Condition Monitoring System

Beitong Tian¹, Kuan-Chieh Lu², Ahmadreza Eslaminia², Yaohui Wang¹, Chenhui Shao², Klara Nahrstedt¹

¹Coordinated Science Laboratory, ²Department of Mechanical Science and Engineering

University of Illinois at Urbana-Champaign, Champaign, USA

{beitong2,kclu3,ae15,yaohuiw2,chshao,klara}@illinois.edu

Abstract—Ultrasonic welding machines play a critical role in the lithium battery industry, facilitating the bonding of batteries with conductors. Ensuring high-quality welding is vital, making tool condition monitoring systems essential for early-stage quality control. However, existing monitoring methods face challenges in cost, downtime, and adaptability. In this paper, we present WeldMon, an affordable ultrasonic welding machine condition monitoring system that utilizes a custom data acquisition system and a data analysis pipeline designed for real-time analysis. Our classification algorithm combines auto-generated features and hand-crafted features, achieving superior cross-validation accuracy (95.8% on average over all testing tasks) compared to the state-of-the-art method (92.5%) in condition classification tasks. Our data augmentation approach alleviates the concept drift problem, enhancing tool condition classification accuracy by 8.3%. All algorithms run locally, requiring only 385 milliseconds to process data for each welding cycle. We deploy WeldMon and a commercial system on an actual ultrasonic welding machine, performing a comprehensive comparison. Our findings highlight the potential for developing cost-effective, high-performance, and reliable tool condition monitoring systems.

Index Terms—Tool Condition Monitoring, Data Acquisition System, Concept Drift, Edge Computing

I. INTRODUCTION

Ultrasonic welding machines (UWM) play a critical role in the lithium battery industry, as they are used to bond batteries with conductors through a process known as the welding cycle. The welding cycle involves several steps, including setup, preparation, welding, cooling, and post-welding operations. The welding phase, highlighted in the green box in Fig. 1(a), is the most crucial step. During this phase, the horn presses two conductor pieces onto the anvil and strikes them with a frequency of 20kHz for about one second, bonding the conductors. High-quality welding is essential. Otherwise, the entire battery set may become unusable. Welding quality is influenced by factors such as tool condition, materials used, conductor surface condition, welding machine parameters, and the human factor. Among these factors, tool condition is the most critical, making UWM tool condition monitoring systems vital for early-stage quality control.

Various UWM tool condition monitoring methods have been extensively researched in academia. For instance, 3D scanned images of the horn and anvil can be used to inspect tool conditions directly. This approach, known as an offline method, is the most straightforward way to assess wear but requires specialized camera equipment and taking the horn

and anvil out of the welding machine, causing significant cost and downtime. Another research focuses on online methods that indirectly monitor UWM conditions by gathering and analyzing information from multiple sensors attached to or near the UWM. For example, [1] employs acoustic emission (AE), power, LVDT (linear velocity displacement transducer), and microphone sensors to collect multi-modal data during the welding phase. This data is then used in a supervised learning fashion to classify tool, material, and surface conditions or their combinations. While this method offers good classification accuracy and minimal downtime, it relies on commercial systems, specifically expensive industrial-grade data acquisition systems (costing over \$3,500) and hand-crafted features, which may not be optimal. Moreover, the method does not account for the influence of concept drift on accuracy. Concept drift describes a practical issue in data-driven methods, where testing data deviates from training data due to changes in time or environment, resulting in decreased testing phase accuracy. A naïve solution involves retraining the model for the new context. However, the substantial labor and time required for data collection and labeling, as well as the difficulty in determining when to retrain, render this approach impractical.

In this paper, we introduce **WeldMon**, a cost-effective ultrasonic **W**elding machine condition **M**onitoring system that can run on the edge device in a standalone way and provide robust and accurate monitoring results in real-time. We ingeniously utilize off-the-shelf sensors, audio ADCs (analog to digital converters), and single-board computers to create a data acquisition system that is significantly more affordable while meeting the specifications required for UWM condition monitoring. We convert multi-modal sensory data collected during each welding phase into a multi-channel image and employ neural network models used for computer vision tasks for feature extraction. The auto-generated features, together with hand-crafted features, are then used for tool condition classification. We design three classification tasks to evaluate our method under realistic scenarios and compare it with various algorithms. Additionally, we assess the differences between WeldMon and a baseline commercial system, thoroughly testing the optimal sensor combinations and the necessity for data augmentation.

In summary, our work has the following contribution:

(1) We build a cost-effective data acquisition system for

UWM condition monitoring. The system’s price (as low as \$120) is more than 20 times less than the widely used system in academics ($> \$3500$) with only a 1% accuracy drop when used on the tool condition classification task.

- (2) We propose a novel neural network-based data processing and augmentation pipeline for classifying UWM conditions. Our approach outperforms the previous state-of-the-art method in most test cases, offers greater robustness to context changes, and enables real-time classification on edge devices.
- (3) We implement and deploy WeldMon to a welding machine located in a research lab and comprehensively evaluate our system with real-world collected data.

II. BACKGROUND & SCOPE

A. Potential Factors Causing Concept Drift

In addition to UWM tool condition (new/worn), various factors can influence the readings of sensors monitoring the UWM. In this subsection, we will discuss these factors, and their impact on sensor readings, and provide examples to illustrate the changes.

Welding Parameters: Different welding tasks require specific sets of parameters, such as welding time, amplitude (measured in micrometers), and pressure (measured in Psi). While welding time and pressure may not significantly impact sensor readings, the amplitude can directly affect the readings of all sensors. Different UWM models will cause substantial changes in sensor readings and sensor deployment locations. However, for different UWMs of the same model, based on our experience, sensor readings will barely change as long as sensors are deployed in similar locations.

Workpiece Characteristics: The material (copper/aluminum), shape, and dimensions of the workpieces used in each welding process can vary. However, our experience shows that sensor readings are almost identical regardless of these variations. One critical factor affecting sensor readings is the cleanliness of the workpiece surface. We simulated contaminated surface conditions by dropping cutting fluid on the welding spot and collected accelerometer data under both clean and contaminated conditions. We then visualized the results using a spectrogram, as shown in Fig. 5. We observed a significant change in the sensor reading pattern when the surface was contaminated, regardless of tool condition (new or worn). It’s important to note that these new patterns may not have been seen in the model development phase, potentially leading to incorrect decisions made by the model. In addition to that, in some cases, when the workpiece is contaminated, the spectrograms of new and worn conditions are barely distinguishable.

B. Properties of Sensors and ADCs

Sensors and ADCs are key components in the UWM condition monitoring system. This subsection provides an overview of their properties, as well as how to leverage them for reducing costs.

Sensors are responsible for converting measured physical quantities into corresponding electrical signals, such as voltage. They can be classified into two categories: digital and analog sensors. Digital sensors output digital data, which is converted by an internal ADC, and have limited bandwidth due to the internal ADCs they use compared to analog sensors. Analog sensors, on the other hand, output a scaled analog voltage directly correlated to the measured physical quantity. Manufacturers typically provide a maximum sensor bandwidth recommendation, as oversampling may not yield useful information due to factors such as noise, small amplitude, or other unknown issues caused by oversampling. However, it is possible to modify some specific sensors’ application circuitry and oversample these sensors, thereby extracting valuable information from higher frequency ranges.

ADCs are essential components in DAQ devices, responsible for sampling voltage signals from analog sensors. ADCs used in DAQ devices should accurately sample multiple voltages simultaneously at very high frequencies (up to several hundred thousand hertz) with minimal noise. A general-purpose ADC is commonly the preferred choice for constructing DAQ devices due to its applicability across various scenarios. In addition to general-purpose ADCs, there are specialized ADCs, such as audio ADCs. Designed explicitly for sampling output voltage from microphones, audio ADCs can easily sample at 100 kHz at a lower cost. Although audio ADCs have certain limitations compared to general-purpose ADCs, these limitations do not adversely affect our applications.

C. Scope of WeldMon

In WeldMon, our goal is to develop a UWM condition monitoring system capable of determining the current tool condition (new or worn) after each welding process. We employ one set of new horns and anvils and one worn set to simulate different tool conditions. The system should possess the following features: (1) Affordability and independence from external computing resources, such as remote servers, to facilitate large-scale deployment at a reasonable cost. (2) High performance, particularly a high accuracy. (3) Robustness against potential concept drift, ensuring that the system can be trained with a limited amount of data covering incomplete patterns while maintaining high accuracy with unseen data.

In our system, the factor that poses a challenge to its generalizability is the change in surface conditions, where we simulate a contaminated surface by dropping cutting fluid on the welding spot. As discussed in the previous subsection, numerous factors may vary across different UWM application scenarios, leading to changes in sensor reading patterns. We opt to alter the workpiece surface condition while keeping all other factors constant (material and dimensions of workpieces, UWM model, and welding process parameters), as it presents the greatest challenge. The introduction of cutting fluid can cause the workpiece to slip during welding, leading to more unpredictable and varied pattern changes. Furthermore, simulating contaminated surface conditions is both practical

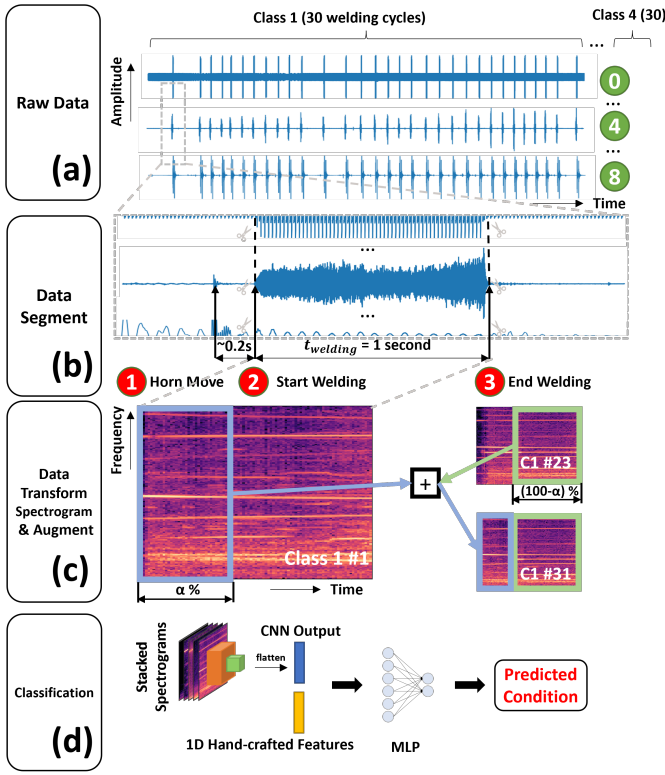


Fig. 2. Weldmon Data Analysis Pipeline.

placed on the workbench under the UWM to capture vibrations from the UWM as they propagate through the workbench.

C. Data Processing Pipeline

Fig. 2 illustrates the data analysis pipeline used in Weld-Mon, from the raw data input to the classification result output. In the following subsections, we explain the major modules and various design choices made to enhance data analysis performance.

Raw Input Data: The raw input data consists of continuous sensory streams, as illustrated in Fig. 2(a). Each second, we obtain $k \times f$ samples, where k represents the number of connected sensors and f denotes the sampling rate of the DAQ device. Instead of using every time window, we only perform data classification on the sensory data collected during the actual welding phase, due to the relevance of this data duration to the tool condition. Qualified data segments are extracted using a data segmentation algorithm.

Data segmentation: The data segmentation algorithm aims to extract data collected during the actual welding phase. A toy example is shown in Fig. 2(b), where the sensory data in the middle is collected from the accelerometer. Our algorithm consists of two stages. In the first stage, we apply a threshold to identify the start time of Horn Move **1**, denoted as t_{hm} . Based on prior knowledge, the horn moves for a maximum of 0.2 seconds. In the second stage, we use another threshold to find the timestamp of Start Welding **2** after $t_{hm} + 0.2$, and the result is denoted as t_{sw} . Since the timestamp obtained from

a threshold-based method will be delayed², we subtract 0.01 second from t_{sw} for a slight adjustment. The End Welding **3** timestamp, denoted as t_{ew} , is $t_{sw} + t_{welding}$, where $t_{welding}$ is a preset UWM parameter, which is set to 1 second in our case. t_{sw} and t_{ew} are then utilized to extract data segments for all sensory streams. The extracted data segment has a shape of $\mathbb{R}^{N \times k}$, where $N = f \times t_{welding}$ represents the number of samples for each sensor in a data segment.

Data Transformation: Since analyzing time-series data in the time-frequency domain has demonstrated potential for better performance compared to the original time domain, we also transform each sensor’s data segment into the time-frequency domain using digital Short Time Fourier Transform (STFT) with proper parameters. We only utilize the magnitude of the STFT result. The outcome is commonly known as a spectrogram, which offers a visual depiction of how the frequency spectrum of the input signal changes over time. We further convert the result to decibel units to reduce the range and reveal more details, using the maximum value of the sensor’s data segment as a reference. The final transformation result for each sensor has a shape of $\mathbb{R}^{T \times F}$, where T denotes the number of time frames and F indicates the number of frequency bins. An example is displayed in Fig. 2(c), where the brightness of the color is directly proportional to the power of a specific frequency at a given time. There is a difference when we transform the data collected by the commercial system since it spans a larger frequency range (to 100 kHz). We use Mel-spectrograms instead of spectrograms since we want to compress the high-frequency range and mainly use the data range around 20 kHz.

Data Augmentation: Data augmentation can enhance data analysis performance when there is insufficient training data to cover the potential feature space. Furthermore, it can help make the trained model more adaptable to unseen data, thereby alleviating the concept drift problem. Despite its many benefits, generating unseen yet realistic samples is a challenge when applying data augmentation. Various data augmentation techniques, such as time warping, adding noise, and time and frequency masking, have been extensively explored in previous works [2], but they may not be optimal for our data. Given the characteristics of the collected data, we found an effective strategy by combining two spectrograms of the same class using a random split ratio to generate a new spectrogram, as described in Algorithm 1. In the algorithm, $A_c^{(b)}$ represents the c^{th} sample of training data A with label b . The augmentation factor controls the quantity of augmented training data by multiplying it with the original training data count. For example, with 100 training samples and an augmentation factor of 5, we will get $(5 \times 100) + 100 = 600$ training samples after data augmentation. A toy example is shown in Fig. 2(c). In this example, we randomly select two spectrograms (#1 and #23) in class 1 and a random split ratio α . The new spectrogram (#31) of class 1 is the concatenation of the first $\alpha\%$ of #1 and the last $(100 - \alpha)\%$ of #23.

²The delay originates from the nonoptimal threshold choice.

Algorithm 1 Data Augmentation

```

1: Input:  $X, y, \text{aug\_factor}, L$   $\triangleright X, y$  are input list and
   label list.  $L = \text{Set of all labels}$ 
2:  $X_{aug} = X, y_{aug} = y$   $\triangleright$  Augmented results
3: for  $l$  in  $L$  do
4:    $X^{(l)}, y^{(l)}$   $\triangleright$  Train data with label equal to  $l$ 
5:    $N_{aug} = \text{aug\_factor} \times \text{len}(y^{(l)})$ 
6:   for  $n$  in  $\text{Range}(N_{aug})$  do
7:      $\alpha \leftarrow \text{rand}(0, 1)$ 
8:      $p, q \leftarrow \text{randInt}[1, \text{len}(y^{(l)})]$   $\triangleright$  No replacement
9:      $X_{new\_1} = X_p^{(l)}[: \lfloor \alpha \times \text{len}(X_p^{(l)}) \rfloor]$ 
10:     $X_{new\_2} = X_q^{(l)}[\lfloor \alpha \times \text{len}(X_q^{(l)}) \rfloor :]$ 
11:     $X_{new} = \text{concatenate}(X_{new\_1}, X_{new\_2})$ 
12:     $X_{aug}^{(l)} = \text{append}(X_{aug}^{(l)}, X_{new})$ 
13:     $y_{aug}^{(l)} = \text{append}(y_{aug}^{(l)}, l)$ 
14:   end for
15: end for
16: return  $X_{aug}, y_{aug}$ 

```

Classification: Spectrograms derived from chosen sensors can be stacked to form a multi-channel image, as illustrated in Fig. 2(d). These images are used as inputs for a Convolutional Neural Network (CNN), an architecture selected for its demonstrated success in image classification tasks. The output of the last convolution layer is flattened to create an auto-generated feature vector, which is then concatenated with a hand-crafted feature vector. This combined vector is fed into a Multilayer Perceptron (MLP) to predict the condition. We name this method a hybrid method. We employ the same set of hand-crafted features as described in [3], owing to their reported strong performance. Apart from CNNs, we also experimented with Convolutional Recurrent Neural Networks (CRNNs), which are anticipated to perform better when capitalizing on the temporal information present in spectrograms. However, in our dataset, CRNNs were not as effective, likely due to the limited temporal information available in the spectrograms.

IV. IMPLEMENTATION

In this subsection, we describe the hardware and software implementation details for WeldMon and the commercial system, as well as the data collection process. We open-source our hardware and software implementation, and all resources will be found on GitHub at https://github.com/beitong95/WeldMon_Public.git.

WeldMon Hardware: The assembled system is depicted in Fig. 1(b). Each sensor is utilized with a custom printed circuit board (PCB), designed using Eagle software and manufactured by JLCPCB. The edge device consists of a Raspberry Pi 4, a Respeaker audio accessory HAT, and a customized connector board. The 3D-printed enclosure for power sensors and the DAQ device, and the sensor mounting base for the accelerometer are designed with Fusion 360 and printed using a Creality Ender 3 3D printer. Shielded 3.5 mm audio cables are employed to connect sensors to the edge device, and data is

TABLE I
HARDWARE IMPLEMENTATION DETAILS

System	Device	Model	Price (\$)
WeldMon	① & ② Power	DRV425	10
	④ Accelerometer	ADXL335	15
	⑥ Microphone	ICS-40300	5
	⑧ Geophone	SM-24	60
	DAQ Device	R-Pi4 + Respeaker Voice HAT	94
	Total		<200
Commercial	① Power	Internal	
	③ LVDT	Internal	
	⑤ Acoustic Emission	R15 α	500
	⑦ Microphone	GRAS 40 PP	700
	⑨ Pressure	Internal	
	DAQ Device	NI USB 6361	2561
Total		>3500	

sampled at a 48 kHz rate with 16-bit sample width. WeldMon utilizes a power outlet as its energy source, which is readily available in most welding workspaces. Additional details, such as sensor type, model, and price, can be found in Table I.

Commercial Hardware: The data acquisition (DAQ) device used is from National Instruments. The power sensor, pressure sensor, and LVDT sensor are internal sensors, and their data is read by the NI DAQ through a customized interface on the UWM. Sound signals are collected by a GRAS 40 PP microphone, powered and amplified by a GRAS 12AL. The acoustic emission sensor, R15 α , uses a preamplifier to amplify the signal so it falls within NI DAQ’s measurement range. Sensors are connected to the NI DAQ using Dupont cables and are sampled at 200 kHz.

UWM and Workpiece Parameters: In our experiment, we employed a Branson Ultraweld L20 model as the ultrasonic welding machine (UWM). We set the operating parameters as follows: pressure at 50 Psi, amplitude at 40 μm , and welding duration at 1 second. The copper workpieces used in the study measured 1 inch in width, 2 inches in length, and had a thickness of 0.008 inches.

Software and Training Setup: The WeldMon data collection software module is developed using Python. Meanwhile, the data collection software for NI DAQ is programmed in MATLAB. We implemented data processing pipelines for both systems in Python.

Our workstation for model training is equipped with an Intel Core i9-10900X CPU @ 3.70GHz, 64 GB RAM, and an Nvidia RTX3080 GPU. We employ the basic CNN architecture without any fine-tuning to the neural network’s structure, which consists of four convolution layers, and three fully connected layers (roughly 11 million parameters). We experiment with popular CNN architectures, such as ResNet-50, but observed inferior results compared to using basic CNN architecture. The Adam optimizer with a 4e-4 learning rate is used for training, with early stopping based on training accuracy and a learning rate reduction strategy. We utilize a batch size of 32 and a maximum of 100 epochs, with the typical training time for each model being under one minute. Evaluation takes place on the same workstation, except for

TABLE II
TOOL AND SURFACE CONDITION EXPLANATION

Condition	Explanation
New	The horn and anvil are new (< 1000 usage times).
Worn	The horn and anvil are worn (> 1000s usage times).
Clean	The workpiece surface is clean.
Contaminated	The workpiece has cutting fluid drops on its surface.

algorithm latency testing, which is performed on the Raspberry Pi 4.

Data Collection: In our study, we focus on two tool conditions and two workpiece surface conditions, as described in Table II. We install WeldMon and the commercial system on the same UWM and perform 30 welding cycles for each combination of tool and surface conditions (New + Clean, New + Contaminated, Worn + Clean, and Worn + Contaminated). This procedure yields two datasets for each system containing sensory data from the same 120 welding cycles across four distinct classes. The data are then processed using the data processing pipeline, as detailed in Section III-C. The four classes can be combined for various classification tasks. For instance, if the objective is to classify the tool condition, we can merge the data from New + Clean and New + Contaminated classes and assign a new class label, "New," which would be the same for data in the worn condition.

V. EVALUATION

In the upcoming evaluation section, we aim to address the following key questions:

- What are the optimal sensor combinations for UWM condition monitoring in each system?
- How do data augmentation and the volume of augmented data impact classification accuracy?
- Does our classification method outperform existing approaches?
- Is WeldMon a viable replacement for Commercial system?

Task Setup: We design three classification tasks based on the collected data to comprehensively evaluate the effectiveness of our system. Task 1 is a multiclass classification of mixed tool and surface conditions. Task 2 and Task 3, on the other hand, focus solely on binary classification of tool conditions, ignoring the surface condition. Task 2 is trained using data from all mixed conditions, while Task 3 is trained only with New + Clean and Worn + Clean data. To simulate the common concept drift problem in real-world scenarios, we also test Task 3 with data collected from the Contaminated condition. Task 1 presents a challenge due to its multiclass classification nature, while Task 3 is even more challenging as it requires the model to accurately classify unseen data.

Evaluation Process & Metrics: For each task and parameter setting (sensor combination, augmentation factor, classification method, etc.), we begin by dividing the dataset into a training set and a held-out testing set, using an 80:20 ratio³. Next, we perform stratified repeated cross-validation (CV) on the

³We use the same random state when splitting the data to make sure the training and testing datasets are the same when we change other parameters.

training set. During this process, we augment the training folds according to a predetermined augmentation factor before training each fold. Following cross-validation, we train a model using the entire training set (also augmented based on the augmentation factor) and evaluate it on the held-out testing set. This yields two sets of accuracy measurements: the average cross-validation accuracy, accompanied by its standard deviation, and the final testing accuracy. While the average cross-validation accuracy and its standard deviation are sufficient for comparing various model designs, we also report the testing accuracy to provide a more comprehensive and robust evaluation of the model's performance.

Baseline Methods: To assess the effectiveness of our proposed classification method, we compare our method with a state-of-the-art method for UWM condition monitoring [3]. This method employs DWT (Discrete Wavelet Transform) to extract multiple features from the data. A multi-layer fully connected neural network is then used to predict the condition based on selected features. We implement the baseline method following the algorithm described in [3]. We also implement a CNN-only method where we remove the handcrafted features used in Fig. 2(d).

Task 1 can also be solved by ensemble learning, combining outputs of two binary classifiers, but the result is not as good as using a multiclass classifier based on our experiment results.

A. Identifying Optimal Sensor Combinations

For each system, we assess all possible sensor combinations (31 in total) and their corresponding accuracies. For each combination, we train and test our hybrid classification model using data from the selected sensors to determine accuracy. The augmentation factor is set to 0, and cross-validation repetition is 1. We rank sensor combinations based on the cross-validation LCB⁴ (Lower Confidence Bound), as shown in Fig. 3. It is evident that the accuracies of both systems are sensitive to changes in sensor combinations, highlighting the significance of identifying optimal sensor configurations for improved performance. We also rank the sensor combinations for the other two baseline methods to find sensor combinations that perform well in all three classification methods⁵. For the WeldMon system, we select Accelerometer ④ and Microphone ⑥ as the best sensor combination, as it ranks among the top 4 for all classification methods. For the Commercial system, the optimal sensor combination includes Power ①, Acoustic Emission ⑤, and Microphone ⑦, as it stably ranks within the top 5 for all classification methods. These best sensor combinations will be used for subsequent evaluations.

Several intriguing observations can be made from the Fig. 3. Using a single sensor in WeldMon, such as an accelerometer or a microphone, yields excellent results, suggesting the potential for removing some sensors to reduce costs and save space in WeldMon (below \$120). It can be seen that adding more

⁴Calculated by cross-validation accuracy mean - 1.96 standard deviations

⁵Due to page limitations, the other two images can be found in our GitHub repository.

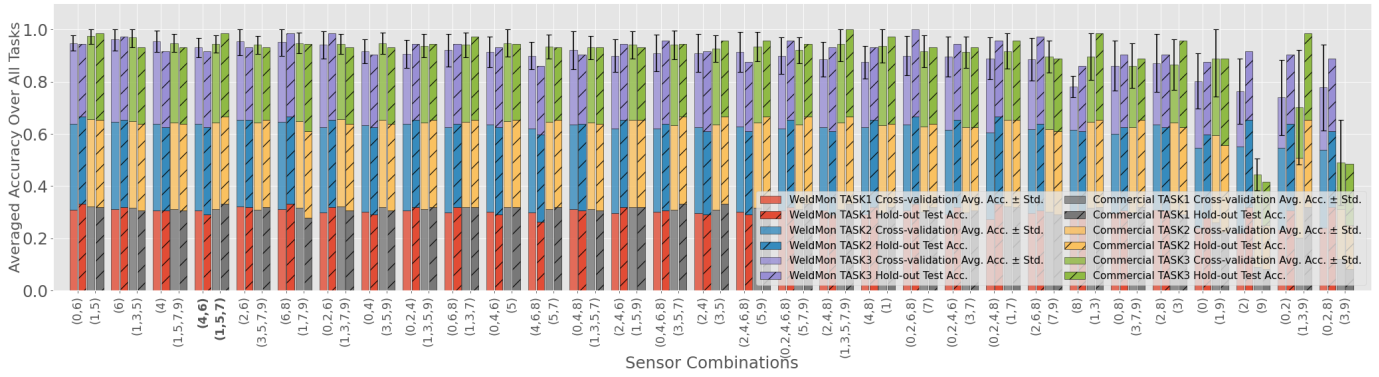


Fig. 3. Average Classification Accuracy Across All Tasks for Different Sensor Combinations. The x-axis shows the combination of sensor IDs (**bolded** ones indicate the selected sensor combinations), which are the same as those used in Fig. 1.

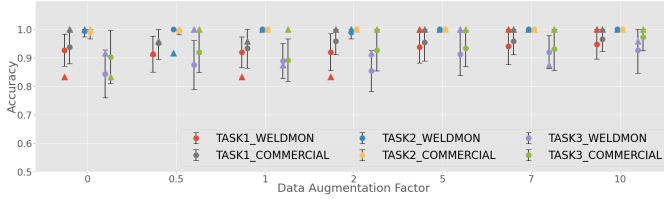


Fig. 4. Error-bar plot of Classification Accuracy under Different Data Augmentation Factors. The dots show the average cross-validation accuracy. The Upward-pointing triangles show the accuracy tested on the held-out data.

sensors or replacing existing ones may not significantly enhance performance, as demonstrated by combinations (4) and (4, 6), since the new sensory stream might be correlated with the original one. Using incorrect sensors only can drastically reduce performance, such as Geophone and Power sensors in WeldMon and LVDT and Pressure sensor in the Commercial System, as they all show bad accuracy in Fig. 3. Fortunately, combining poor sensors with good ones does not considerably diminish performance, as demonstrated by combinations (0, 2, 4, 6, 8) and (0, 2, 8).

B. Effectiveness of Data Augmentation

We test our system under different data augmentation factors ranging from 0 to 10 and report the averaged accuracy and standard deviation of 3 repetitions of 6-fold cross-validation and also the final testing accuracy as shown in Fig. 4. We can find a clear trend that the results of all tasks of both systems improve and get more reliable, and the accuracy gap between WeldMon and the commercial system gets smaller with the increment of the augmentation factor. When the augmentation factor reaches 5, both systems reach their optimal performance and have the smallest final test accuracy differences. More augmentation will not help to improve the performance significantly. Recall in Task 3, both systems are challenged with the concept drift problem. With the data augmentation factor set as 10, the averaged accuracy of cross-validation improves by 8.3 % and 6.9 % for WeldMon and Commercial system, respectively which proves the effectiveness of the proposed data augmentation method in alleviating the concept drift problem. For Task 1, the final test accuracy improves by 16.7 % to 100 % for WeldMon with the augmentation factor set

TABLE III
ACCURACY & LATENCY UNDER DIFFERENT METHODS

System	Task	Method	CV ¹	Test	Time ² (ms)
WeldMon 48kHz	Task1	Hybrid	0.941 (0.057)	0.958	383 (764)
		DWT	0.910 (0.079)	0.917	265 (607)
		CNN	0.938 (0.059)	1.000	266 (627)
	Task2	Hybrid	0.997 (0.014)	1.000	386 (764)
		DWT	0.983 (0.035)	1.000	263 (681)
		CNN	1.000 (0.000)	1.000	265 (682)
Task3	Hybrid	0.906 (0.063)	0.875	384 (764)	
	DWT	0.920 (0.072)	1.000	262 (612)	
	CNN	0.913 (0.073)	0.917	263 (649)	
Commercial 200kHz	Task1	Hybrid	0.955 (0.072)	0.958	
		DWT	0.899 (0.076)	0.917	
		CNN	0.951 (0.064)	1.000	
	Task2	Hybrid	1.000 (0.000)	1.000	
		DWT	0.986 (0.033)	1.000	
		CNN	1.000 (0.000)	1.000	
Task3	Hybrid	0.951 (0.074)	1.000		
	DWT	0.851 (0.066)	0.833		
	CNN	1.000 (0.000)	1.000		

¹ Accuracy of 3 repetitions of 6-fold cross-validation, with results reported as mean (standard deviation).

² Mean (Max) computation time per sample over 300 experiments in ms.

to 5 or more which shows the great impact of the proposed data augmentation method towards the classification accuracy of WeldMon.

C. Comparing Different Classification Methods

In this experiment, we set the augmentation factor to 5 and employ the optimal sensor combination for each system. We then compare the accuracy of our hybrid method and two baseline methods under different systems and tasks. As shown in Table III, our method shows similar performance on both systems compared to the CNN-only method and outperforms the DWT method in most cases. During the experiment, we also find the performance of our method is less sensitive to different sensor combinations compared to the CNN-only method. Also, our method is easier to converge but the CNN-only method may not converge in some cases.

To compare the computation time of the proposed and baseline methods, we run 300 data processing cycles (from data transformation to the end of classification) on a Raspberry Pi 4 with 4 GB RAM, while simultaneously collecting data. For each task and model combination, we report the mean and maximum computation time in Table III. Results show

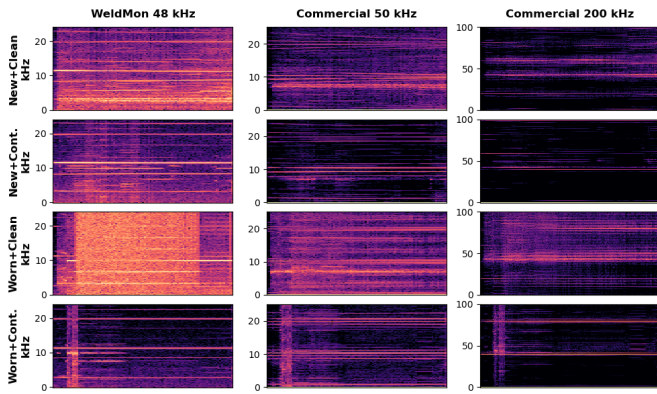


Fig. 5. Sample spectrograms of WeldMon (accelerometer), Commercial System (acoustic emission sensor), and Commercial System with downsampled data under various mixed conditions. Each row corresponds to a specific mixed condition, while each column indicates the system name and its corresponding sampling rate. The x-axis spans 1 second.⁷

TABLE IV
ACCURACY OF DIFFERENT SYSTEMS

System Sampling Rate	Task1		Task2		Task3	
	CV ¹	Test	CV	Test	CV	Test
WeldMon 48kHz	0.94	0.96	1.00	1.00	0.91	1.00 ²
Commercial 200kHz	0.94	0.96	1.00	1.00	0.92	1.00
Commercial 50kHz	0.97	1.00	1.00	1.00	0.96	1.00

¹ Averaged accuracy of 3 repetitions of 6-fold cross-validation.

² The test accuracy is different from Table III may be caused by randomness in data augmentation.

that the proposed hybrid method has longer computation time compared to the other two baseline methods, due to extra feature extractions and more complex neural network model. The observed latencies are acceptable, considering that the minimum interval between two welding processes is much longer than the average computation time. In future work, we aim to further reduce data processing time, enabling our algorithm to run on devices with more limited computing resources and handle additional sensory streams or more complex algorithms.

D. Comparing WeldMon with the Commercial System

Despite using optimal configurations, a significant accuracy disparity persists between WeldMon and the commercial system in Task 3, as shown in Fig. 4 and Table III. Our goal is to investigate the root cause of this discrepancy. We begin by visually comparing spectrograms from different systems. Fig. 5 presents sample spectrograms for accelerometer and acoustic emission sensor data, as well as downsampled acoustic emission sensor data at 50 kHz. The commercial system’s spectrograms display unique information above 24 kHz, which may contribute to the accuracy difference. Comparing WeldMon 48 kHz and Commercial 50 kHz, the commercial system’s spectrograms exhibit more detail and less noise, suggesting sensor specification differences could contribute to the accuracy gap.

⁷Cont. is short for contaminated. For a more accurate comparison, linear spectrograms are used for the commercial system, rather than Mel-spectrograms which are used in other evaluations.

We then conduct a quantitative analysis using a specially designed experiment. To ensure a meaningful comparison, both systems must use identical sensor types. We select the accelerometer and acoustic emission sensor, which monitor anvil vibrations, and a pair of microphones for each system. We also downsample the commercial system’s data to 50 kHz to evaluate the impact of the maximum frequency limit. We apply our data analysis pipeline to the data from the chosen sensors (with an augmentation factor of 5) and present the findings in Table IV. The results reveal a substantially reduced accuracy gap between WeldMon and the commercial system sampling at 200 kHz, emphasizing the importance of the additional power sensor used in Sec. V-C. Interestingly, the commercial system sampling at 50 kHz demonstrates superior performance, indicating that the maximum frequency limit is not the main factor behind the accuracy discrepancy. These observations lead us to conclude that the primary source of the accuracy gap lies in the sensors themselves, whether in the sensor type or their specifications. Although sensor differences are challenging to overcome, we can mitigate them with advanced algorithms, sensor fusion techniques, or by adding new sensors, which we intend to explore in our future work.

VI. RELATED WORK

This paper presents a cost-effective welding machine monitoring system that runs on an edge device, delivering real-time, accurate, and reliable results. We review cost-effective data acquisition systems, DNN-based machine condition monitoring, and solutions for handling concept drift.

A. Cost-effective DAQ systems:

The deployment of machine learning-based monitoring systems relies heavily on the cost of data acquisition devices. Traditional systems used for UWM are expensive, hindering large-scale deployment. Numerous studies have investigated low-cost data acquisition devices for diverse applications. For instance, [4] developed a cost-effective Arduino-based DAQ system for automotive dynamics, which showed only a 2.19 percent error rate compared to traditional vibration acquisition methods. Despite its success, single-sensor DAQ systems have limitations, as discussed in Sayyad et al. [5], leading to a preference for multi-sensor approaches. [6] introduced an affordable multi-sensor DAQ system employing the 1-Wire Bus for large-scale indoor environmental monitoring. However, due to its limited sampling frequency, this system is not suitable for applications such as UWM, which operates at 20 kHz. To address this, Soto-Ocampo et al. [7] designed an affordable, high-frequency DAQ system, diagnosing a bearing test rig, which is five times cheaper than myDAQ from National Instruments. Another challenge in low-cost data acquisition systems is real-time or near real-time processing. [8] presented an IoT-based intelligent low-cost system for vehicle data acquisition, offering near real-time data processing at a lower cost (up to 13 times cheaper) compared to industrial devices. In ultrasonic welding, Lu et al. conducted case studies on reducing the cost of building a UWM condition monitoring system by

decreasing the sampling rate and the number of sensors, but they only simulated the result on a high-cost DAQ system and did not implement an actual low-cost system. Moreover, their work relied on hand-crafted features for data processing, which may not be optimal and robust to context changes. Thus, developing a low-cost DAQ system holds significant potential for various applications.

B. DNN-based Machine Condition Monitoring

Tool Condition Monitoring (TCM) has gathered significant research interest over the past few decades due to its critical role in the manufacturing industry [1]. Tool wear mechanisms are influenced by varying process parameters and conditions [9], complicating the development of effective TCM systems for certain manufacturing processes. Data-driven TCM methods have utilized fuzzy logic systems, Bayesian networks, decision trees, support vector machines (SVM), and artificial neural networks (ANN). Recently, deep learning techniques have emerged as a more effective approach. For instance, Zhao et al. [10] introduced a deep learning model, Convolutional Bi-directional Long Short-Term Memory Networks (CBLSTM), for tool wear testing in CNC milling.

Online DNN-based TCM research for UWM is limited, mainly due to its high oscillation frequency and short welding cycle. In [11], the authors employed a convolutional neural network for joint quality prediction in UMW, showcasing robustness to tool conditions. Meanwhile, Lu et al. used a multi-layer perceptron (MLP) classifier for identifying welding disturbances related to tool and material surface conditions. In this paper, we transform multimodal sensory data from welding phases into multi-channel images, then use a CNN for feature extraction and an MLP for classification.

C. Addressing Concept Drift in Monitoring Systems

Concept drift poses a significant challenge in supervised machine learning-based monitoring, particularly in real-world applications with frequently changing contexts. Various studies have proposed solutions for this issue. For instance, Yang et al. [12] developed CADE, a system using a contrastive auto-encoder and distance-based explanation method to enhance supervised classifiers in security contexts. In manufacturing condition monitoring, Shi et al. [13] introduced a contrastive generalization net (RFACGN) for intelligent fault diagnosis under unseen machine and operational conditions. This net demonstrates excellent generalization ability and diagnostic efficiency compared to other state-of-the-art methods. Lin et al. [14] proposed an ensemble learning algorithm for offline classifiers, addressing concept drifts and imbalanced data in three-stage condition-based maintenance (CBM). For online applications, Zenisek et al. [15] presented a method to detect concept drift in data streams as an indicator of defective system behavior in industrial settings, validating their approach on synthetic and real-world data sets. These studies highlight the importance of addressing concept drift in machine learning-based monitoring systems, especially in manufacturing tool condition monitoring. We propose a data augmentation method

specially used for the UWM monitoring data to alleviate the concept drift problem.

VII. CONCLUSION

This paper introduces WeldMon, the first cost-effective autonomous system for real-time UWM condition monitoring. We detail WeldMon's design, implementation, and deployment, emphasizing its cost-effectiveness, superior accuracy, and robustness to context changes. The results indicate that WeldMon offers a practical, effective, and reliable solution for real-world applications, paving the way for future advancements in cost-efficient and robust condition monitoring systems.

REFERENCES

- [1] Q. Nazir and C. Shao, "Online tool condition monitoring for ultrasonic metal welding via sensor fusion and machine learning," *Journal of Manufacturing Processes*, vol. 62, pp. 806–816, 2021.
- [2] D. S. Park, W. Chan, Y. Zhang, C.-C. Chiu, B. Zoph, E. D. Cubuk, and Q. V. Le, "SpecAugment: A simple data augmentation method for automatic speech recognition," *arXiv preprint arXiv:1904.08779*, 2019.
- [3] Y. Meng and C. Shao, "Physics-informed ensemble learning for online joint strength prediction in ultrasonic metal welding," *Mechanical Systems and Signal Processing*, vol. 181, p. 109473, 2022.
- [4] A. González, J. L. Olazagoitia, and J. Vinolas, "A low-cost data acquisition system for automobile dynamics applications," *Sensors*, vol. 18, no. 2, p. 366, 2018.
- [5] S. Sayyad, S. Kumar, A. Bongale, P. Kamat, S. Patil, and K. Kotecha, "Data-driven remaining useful life estimation for milling process: sensors, algorithms, datasets, and future directions," *IEEE Access*, vol. 9, pp. 110255–110286, 2021.
- [6] B. Tian, Z. Yang, H. Moeni, R. Gupta, P. Su, R. Kaufman, M. McCol-lum, J. Dallesasse, and K. Nahrstedt, "Senselet++: A low-cost internet of things sensing platform for academic cleanrooms," in *2021 IEEE 18th International Conference on Mobile Ad Hoc and Smart Systems (MASS)*, pp. 90–98, IEEE, 2021.
- [7] C. R. Soto-Ocampo, J. M. Mera, J. D. Cano-Moreno, and J. L. Garcia-Bernardo, "Low-cost, high-frequency, data acquisition system for condition monitoring of rotating machinery through vibration analysis-case study," *Sensors*, vol. 20, no. 12, p. 3493, 2020.
- [8] J. P. Bedretchuk, S. Arribas García, T. Nogiri Igarashi, R. Canal, A. Wedderhoff Spengler, and G. Gracioli, "Low-cost data acquisition system for automotive electronic control units," *Sensors*, vol. 23, no. 4, p. 2319, 2023.
- [9] Z. Li, R. Liu, and D. Wu, "Data-driven smart manufacturing: Tool wear monitoring with audio signals and machine learning," *Journal of Manufacturing Processes*, vol. 48, pp. 66–76, 2019.
- [10] R. Zhao, R. Yan, J. Wang, and K. Mao, "Learning to monitor machine health with convolutional bi-directional lstm networks," *Sensors*, vol. 17, no. 2, p. 273, 2017.
- [11] Y. Wu, Y. Meng, and C. Shao, "End-to-end online quality prediction for ultrasonic metal welding using sensor fusion and deep learning," *Journal of Manufacturing Processes*, vol. 83, pp. 685–694, 2022.
- [12] L. Yang, W. Guo, Q. Hao, A. Ciptadi, A. Ahmadzadeh, X. Xing, and G. Wang, "CADE: Detecting and explaining concept drift samples for security applications," in *USENIX security symposium*, pp. 2327–2344, 2021.
- [13] Z. Shi, J. Chen, X. Zhang, Y. Zi, C. Li, and J. Chen, "A reliable feature-assisted contrastive generalization net for intelligent fault diagnosis under unseen machines and working conditions," *Mechanical Systems and Signal Processing*, vol. 188, p. 110011, 2023.
- [14] C.-C. Lin, D.-J. Deng, C.-H. Kuo, and L. Chen, "Concept drift detection and adaption in big imbalance industrial iot data using an ensemble learning method of offline classifiers," *IEEE Access*, vol. 7, pp. 56198–56207, 2019.
- [15] J. Zenisek, F. Holzinger, and M. Affenzeller, "Machine learning based concept drift detection for predictive maintenance," *Computers & Industrial Engineering*, vol. 137, p. 106031, 2019.